CALCULATION OF SHUTTLE BASE HEATING ENVIRONMENTS AND COMPARISON WITH FLIGHT DATA

Terry F. Greenwood and Young C. Lee
NASA Marshall Space Flight Center
Marshall Space Flight Center, Alabama

Robert L. Bender
REMTECH, Incorporated
Huntsville, Alabama

Robert E. Carter
Lockheed Missiles and Space Company
Huntsville, Alabama

SUMMARY

The techniques, analytical tools, and experimental programs used initially to generate and later to improve and validate the Shuttle base heating design environments are discussed in this paper. In general, the measured base heating environments for STS-1 through STS-5 were in good agreement with the preflight predictions. However, some changes were made in the methodology after reviewing the flight data. This paper describes the flight data, compares preflight predictions with the flight data, and discusses improvements in the prediction methodology based on the data.

INTRODUCTION

The Space Shuttle base heating environment is a combination of SSME and SRM plume radiation, freestream air convective cooling, and reversed plume flow convective heating. Each base region component receives differing levels of radiation and convective heating depending upon its location relative to the plumes, base gas absorption, structural blockage, general base configuration, and local surface temperature. The radiation environment varies with the plume shape, and the incident radiation to any base location depends upon the emission/absorption and afterburning characteristics of each contribution plume and by the magnitude of attenuation of the base region gases. Convective cooling affects hot base surfaces during initial first-stage flight as cool freestream air is drawn through the base by the aspirating action of the plumes. At higher altitudes when the plumes become highly expanded and interact, hot gases from the SSME and SRM nozzle boundary layers are reversed into the base with resultant base convective heating to most base surfaces.

The Shuttle base configuration during 1st- and 2nd-stage ascent is shown in Figure 1. Those surfaces closest to the plumes - the SRB skirt trailing edge, the body flap trailing edge, and the SSME aft hat bands - receive the highest levels of radiation, approximately 16 Btu/ft^{2}sec at liftoff. Convective heating is most intense in the center heat shield region of the orbiter and in the

upper center of the ET dome where levels of heating of 8 Btu/ft^2sec were measured at approximately 100,000 ft altitude. A spike in heating occurs during the last few seconds of SRM shutdown, producing an increase in radiation and convection well above nominal levels. Peak total heating during this period can exceed 25 Btu/ft^2sec at some locations.

A typical heating environment history at the center of the LH_2 tank aft dome is shown in Figure 2. Photographs of the plumes at several altitudes encompassing the full spectrum of base heating variations are presented in Figures 3 through 6. The thermal environment for the first 70 to 80 seconds of flight is dominated by SRM radiation. For the first 30 seconds, the plume radiation to the base surface is attenuated by base region outgassing. Beyond 30 seconds, radiation increases to near sea-level magnitudes followed by a gradual decrease until about 90 seconds (70,000 feet). Note also that convective cooling of the ET base occurs during the first 70 seconds of first-stage flight. Above 90 seconds, the plumes begin to strongly interact and recirculate hot gases with the peak convective effect occurring at about 75% SRM thrust and 100 seconds (100,000 feet). The SRM shutdown spike, noted at 128 seconds (166,000 feet), is visible in the plume photograph shown in Figure 6.

A more detailed look at the effect of the various flight events on the base heating environment can be seen in Figure 7. The environment shown in Figure 7 was measured in the center of the orbiter heat shield. This location was selected because it experiences heating throughout ascent and is sensitive to the various engine operational variations. As seen in this figure, the radiation environment early in flight is not significantly influenced by ignition, the roll maneuver, and throttling down to 65% thrust for max q. Radiation levels are reduced with altitude since plume gas temperatures decrease at a rate faster than the view factor of the expanding plume boundary increases. Freestream air convective cooling reduces total base heating until the plume boundaries intersect and recirculate rocket exhaust gasses toward the base at approximately 70 seconds. Convective heating, shown as the shaded areas in Figure 7, is dramatically affected by SRM thrust tailoff. If tailoff did not occur after 100 seconds, convective heating would continue to increase with increasing altitude during 1st-stage flight. Both radiation and convection increase during SRM shutdown, but the predominant effect at this base location is a dramatic increase in radiation. Both radiation and convection are constant during the high-altitude steady SSME performance period of 2nd-stage flight. Convection declines sharply when the SSMEs throttle down to 3g after 450 seconds. All base heating to the orbiter heat shield becomes negligible after main engine cut-off (MECO).

PREFLIGHT METHODOLOGY

Because of its extended reuse capability and flyback operational capability, the Shuttle thermal protection system (TPS) must be adequate but not grossly overdesigned. Any excess weight designed into the system because of an overdesigned TPS directly impacts payload capability and operating costs. Therefore, an extensive effort to accurately predict the ascent base heating environment was undertaken early in the Shuttle program. A paper[1] documenting the preflight Shuttle base heating methodology was presented at the JANNAF 10th Plume Technology Meeting. Important features of the preflight methodology are

summarized in the following paragraphs. Radiation and convective heating components of the total environment prediction utilize different methods and are computed independently.

Radiation

SRM - The sea-level SRM plume radiation math model was originally based on experimental data taken on the Titan IIIC solid motors[2], geometrically scaled to the SRM size as shown in Figure 8(a). This sea-level model was subsequently updated based on ground tests of the SRM. In January 1977 (DM-1) and February 1978 (DM-2) the SRM was statically fired at the Thiokol Test Range in Utah (5000 ft elevation). Narrow-view-angle radiometer data were obtained along the plume centerline from the exit plane of the nozzle on DM-2. On both tests, wide-angle radiometer data were obtained at positions that simulated locations on the Shuttle vehicle. From these data, a new sea-level plume emissive power radiation model was developed.[3] This model consisted of a 12° cone-cylinder shape with the emissive power (E) changing along the centerline as shown in Figure 8(b).

Subsequent testing of the SRM at the Thiokol Utah Test Range (QM-2 and QM-3 in October 1979 and February 1980) provided narrow-view-angle radiometer measurements near the nozzle exit plane slightly higher than measurements taken on DM-1 and DM-2. Updating the emissive power of the first four plume segments of the SRM math model to values of $E = 70$, 59, 57, and 53 Btu/ft^2sec resulted in the plume model shown in Figure 8(c)[4] and a better correlation of the measured and predicted QM-2 and QM-3 heating rates. A comparison of the SRM plume radiation heating rates to the Shuttle vehicle made with this model (1980 updated model) compared to the older 1979 design model showed only slightly higher heating rates.

With the sea-level plume emissive power math model defined, radiation heating rates to various design points on the Shuttle were calculated using a radiation view factor computer program.[5] Initial predictions assumed no altitude variation. Later predictions (before flight data became available) considered altitude effects using a recently developed Monte Carlo radiation code[6] coupled with detailed, two-phase plume flow field calculations and the plume model shown in Figure 9.[7]

SSME - Radiation heating rates from the SSME plumes were calculated using a modified form of the basic NASA band model gaseous radiation program[8]. An extensive effort was made to correctly model the Mach disk region and the viscous shear layer of the plume (see Figure 10). At low to mid altitudes, the plumes do not interact, so detailed radiation calculations were made for each plume and the environment generated at a given design location by adding the contributions from each plume. The complex three-dimensional flow field occurring at high altitudes when the SSME plumes interact and reverse gases into the orbiter base region was approximated using two-dimensional techniques.[1]

Convection

Unlike radiation predictions, convective base heating predictions were based almost entirely on short duration, hot-firing model test data. Eight

separate base heating tests were conducted to support the convective environment analysis as listed in Figure 11. The basic model used throughout these tests for first-stage condition was a 2.25% version of the fully integrated launch vehicle. These tests utilized short duration techniques that included hot-firing hydrogen-oxygen simulation of the SSME, hot-firing simulation of the booster SRM, and simulated external air flow over the model. The model used for second-stage test conditions was a 4% scale model of the orbiter base region, vertical fin, OMS pod, and body flap, which included hot-firing hydrogen-oxygen simulation of only the SSMEs. These tests were conducted in altitude chambers with no external flow, only a variable chamber back pressure.

During these tests, model heating rates and gas temperatures were measured over a range of simulated altitudes, and all factors affecting convective base heating were parametrically varied to provide a detailed base heating data base. When the flight conditions were established, this data base was used to extract the model heat transfer coefficient corresponding to the specific flight condition. The scaling techniques from model to full scale were based on the Colburn Turbulent Scaling Law. Details of these techniques are provided in Reference 1. Analytical predictions for the mass-averaged base gas recovery temperature were made by estimating the mass flow of exhaust products into the base region and then integrating the total energy flow in the nozzle boundary layer from the nozzle wall to this mass flow rate. Average temperature as a function of boundary layer mass flow is shown in Figure 12 for the exit plane of the SSME.

FLIGHT DATA

Base heating environment data have been measured on the four development flights as well as the first operational flight. A limited amount of data was obtained on STS-1 due to bad instrumentation initially installed on the orbiter and main engines and reduced instrumentation on the ET base. The bad instruments were replaced on STS-2, and a complete base heating data base was obtained on all subsequent flights with the single exception of the SRB data on STS-4, which was lost when the boosters sank following water impact. The flight instrumentation, operating conditions which affect base heating, and typical flight data are described in the following paragraphs.

Flight Parameters and Operating Characteristics

Shuttle flight parameters which influence base heating are: vehicle trajectory (Figure 13), vehicle angle of attack (Figure 14(a)), SRM chamber pressure history (Figure 14(b)), and SSME chamber pressure history (Figure 14(c)). Other flight and operating conditions affecting base heating, but not shown in this paper, include SSME and SRM gimbaling and vehicle side slip. Altitude and SRM thrust decay history have the most impact; other flight and operating conditions have a second-order effect. Model data indicate that SSME gimbaling can have significant effects on orbiter base heat shield 2nd-stage convective heating if the gimbal angles significantly deviate from current baseline nominal. However, on all Shuttle flights to date, the SSME gimbal angles flown on each flight have not varied from this nominal, and the measured flight data have been similar. The SRM and SSME chamber pressure histories shown in Figures 14(b) and 14(c) are typical for all engines for all flights.

The altitude histories during 1st-stage ascent have been remarkably similar on all five flights as have the engine operating conditions. Therefore, it was expected that the measured environments would be similar in magnitudes and trends. Flight-to-flight differences noted in the data are primarily a function of local flow field differences, gage contamination, TPS outgassing, flight-to-flight gage replacement and range changes, etc. The global base region flowfields, plume shapes, gas temperatures, and TPS and instrumentation temperature were generally the same on all flights.

Development Flight Instrumentation

Flight instrumentation to monitor ascent base heating consisted of total calorimeters, radiometers, and gas temperature probes. The number of instruments greatly increased from STS-1 to STS-2 and subsequent flights, and the quality of the measurements was also improved on STS-2 and subsequent flights at some base locations. A variety of different type gages and different mounting and data retrieval systems were used throughout the various base components. With the exception of the gas temperature measurements, the data were generally good, consistent from component to component, and were of significant value in understanding the base heating environments. Total calorimeter sensor temperatures were generally less than 200°F throughout ascent, so the measured total heating rates reflect an essentially cold wall convective component. Gas temperatures were measured for the ET and right SRB; no gas temperature measurements were taken on the orbiter and SSMEs.

Typical Flight Base Heating Data

Complete presentations of all base heating data for STS-1 through STS-5 are presented in References 9 through 13. As mentioned previously in the introductory discussion, the highest radiation heating occurs on aft-facing components at liftoff and during the SRB shutdown spike. Convective heating, which can be determined by subtracting radiation from the total heating at the same location, is often negative (convective cooling) during the early part of flight but generally peaks at the highest altitude where substantial booster thrust still occurs. This convective peak has occurred on all flights to date at approximately 100,000 feet altitude or 100 seconds into flight at a booster thrust level of 75%. Typical heating levels throughout the base region including outboard locations such as the vertical tail, body flap, and wing/elevon trailing edges are listed in Figure 15 at four times during a typical flight when the environments are distinctly different.

Typical heating rate histories for various base components are presented in Figures 16 through 23. The orbiter and main-engine data are characterized by significant heating through main engine cut-off. The SRB and ET aft dome environments terminate at SRB separation. It is apparent that all base components experienced a heating spike during the last seven seconds of SRM shutdown. The SRM plumes become brighter and have greater radiation potential during this time period as propellant residuals and liners are ejected through the nozzle and burn in the plume. All flights have shown significant amounts of luminous gases in the general base region surrounding the ET aft dome immediately following liftoff. These gases are hot SOFI ablation outgases released by the initial radiation heating load. They reduce the heat load by attenuating radiation to the base-region surfaces.

IMPROVED METHODOLOGY

Close examination of the flight data indicates that two changes were necessary in the basic SRM plume radiation prediction methodology. The sea-level radiation model was modified to account for the combustion zone between the SRMs resulting from the outgassing TPS material from the ET base combusting as it flows downstream between the SRM plumes. An altitude correction factor to modify sea-level SRM radiation rates to account for altitude changes was also developed from the flight experience. A discussion of these and other methodology changes is presented in Reference 14.

The Shuttle flight data generally validated the convective methodology. For most base surfaces, the agreement between prediction and flight data was good indicating that the scaling methods were correct. However, at three distinct base locations, the prediction methodology was obviously incorrect. These locations were the upper interior region of the orbiter base heat shield, the upper ET aft dome surface, and the outboard SRB skirt. At the upper heat shield location, the preflight methodology overpredicted convective heating during second stage. Conversely, the methodology underpredicted ET dome and outboard SRB skirt convective heating during the intense recirculation period at the end of first stage boost. Details of the improved methodology are described in the following paragraphs.

Radiation

SRM - Based on flight data from STS-1 and STS-2, the shape of the sea-level emissive power model was changed to a 15° cone with the same emissive powers for each segment as the 1980 design model, shown in Figure 24. The second change consists of the development of an altitude correction factor used to modify the sea-level SRM radiation rates to account for altitude variations (Figure 25). This procedure eliminates the launch stand correction factor that was present in the earlier methodology. The SRM altitude correction factor as depicted in Figure 25 is valid for any Shuttle trajectory (since it is a function of altitude only) except for the SRM shutdown spike, which occurs at the end of the SRM burn. Since this spike is a function of time (i. e., the last 7 seconds of SRM burnout, as shown in Figure 26), it is superimposed on the altitude plot at the appropriate altitude corresponding to 7 seconds before burnout and separation.

SSME - The general approach for calculating SSME plume radiation has not changed since Reference 1 was published. However, improvements in the SSME sea-level flowfield model have been made and incorporated in the model.[15] An improved emissive power SSME plume radiation model was developed from extensive gaseous radiation calculations made with the improved GASRAD computer code. The current SSME sea-level plume radiation model is shown in Figure 27.

Comparison of Preflight and Improved Radiation Methodology - STS-5 flight data are compared with the original design environment predictions (preflight methodology) and the operational flight predictions (improved methodology) in Figures 28 through 32. Each figure presents a comparison at a distinctly dif-

ferent base component location: center of the ET aft dome, the lower left corner of the orbiter heat shield, the SRB aft kick ring, the inboard aft hat band of the lower left SSME, and the sway strut of the ET/orbiter attach structure. For most locations, the improved methodology results in a radiation environment somewhat higher than the earlier design critical review (DCR) design environment and includes the SRM shutdown spike.

Convection

To update the convective heating methodology, flight data were substituted for the nominal model data base for the ET upper dome, SRB aft skirt, and the orbiter upper heat shield. Because the flight data were measured over a relatively narrow range of freestream and operating conditions, model data trends and distributions are retained in the up-dated methodology to encompass all possible flight conditions anticipated in future operational flights. The Shuttle flight data also showed less variation in convective heating over large surfaces, such as the orbiter heat shield, the OMS pod base, and the SSMEs, than had been indicated by the model data.

Original methods to predict base gas recovery temperature are unchanged in the up-dated methodology. No valid base gas temperature measurements were made anywhere in the Shuttle base region during the DFI flights. Gas probes, in general, have large uncertainties and potential errors and for these reasons the conservative gas temperatures derived from analytical methods will be retained.

Comparison of Pre-flight and Improved Convective Heating Methodology - Model data, design predictions (preflight methodology), flight data from STS-4, and the operational flight predictions (improved methodology) are compared for four different base locations in Figures 33 through 36. For some locations, e. g. - the ET dome, the operational flight environment encompasses the flight data and is approximately twice the magnitude of the DCR design environment. Conversely, operational predictions for the upper center region of the orbiter heat shield were substantially reduced from the original DCR environments.

REFERENCES

1. Greenwood, T. F., Seymour, D. C., and Bender, R. L.: "Base Heating Prediction Methodology Used for the Space Shuttle," Proceedings of the JANNAF 10th Plume Technology Meeting, Chemical Propulsion Information Agency, CPIA-29, Volume 2, San Diego, California, December 1977, pp. 253-312.

2. Kramer, O. G.: "Evaluation of Thermal Radiation From the Titan III Solid Rocket Motor Exhaust Plumes," Paper No. 70-842, AIAA 5th Thermophysics Conference, Los Angeles, July 1970.

3. Carter, R. E.: "Space Shuttle SRB Plumes-Thermal Radiation Model," LMSC-HREC TR D568530, Lockheed Missiles & Space Company, Huntsville, Alabama, December 1978.

4. Carter, R. E.: "Improved SRM Plume Radiation Design Heating," LMSC-HREC TN D698084, Lockheed Missiles & Space Company, Huntsville, Alabama, November 1980.

5. Lovin, J. K., and Lubkowitz, A. W.: "User's Manual (RADFAC) A Radiation View Factor Digital Computer Program," LMSC-HREC TN D148620, Lockheed Missiles & Space Company, Huntsville, Alabama, November 1969.

6. Watson, G. H., and Lee, A. L.: "Thermal Radiation Model for Solid Rocket Plumes," Journal of Spacecraft and Rockets, Volume 14, No. 11, November 1977, pp. 641-647.

7. Carter, R. E., and Lee, A. L.: "Space Shuttle SRB Plume Radiation Heating Rate Prediction With Altitude Corrections," LMSC-HREC TM D497262, Lockheed Missiles & Space Company, Huntsville, Alabama, September 1977.

8. Reardon, J. E.: "Prediction of Radiation From the Space Shuttle Main Engine to the Orbiter Base Region," RTR 011B-4, REMTECH, Inc., Huntsville, Alabama, May 1976.

9. NASA/Marshall Space Flight Center: "Space Shuttle STS-1 Final Flight Evaluation Report - Volume II - Base Heating Section VI," July 22, 1981.

10. Greenwood, T. F.: NASA/Marshall Space Flight Center Memo ED33-82-3, "STS-2 Flight Evaluation Report - Base Heating," January 15, 1982.

11. Greenwood, T. F.: NASA/Marshall Space Flight Center Memo ED33-82-25, "STS-3 Flight Evaluation Report - Base Heating," April 25, 1982.

12. Greenwood, T. F.: NASA/Marshall Space Flight Center Memo ED33-82-46, "STS-4 Flight Evaluation Report - Base Heating," August 10, 1982.

13. Greenwood, T. F.: NASA/Marshall Space Flight Center Memo ED33-82-65, "STS-5 Flight Evaluation Report - Base Heating," December 2, 1982.

14. Greenwood, T. F. et al.: "Development of Space Shuttle Base Heating Methodology and Comparison With Flight Data," Proceedings of the JANNAF 13th Plume Technology Meeting, Chemical Propulsion Information Agency, CPIA-357, vol. 1, Houston, Texas, April 1982, pp. 67-82.

15. Reardon, J. E., and Lee, Y.: "Space Shuttle Main Engine Plume Radiation Model," RTR 014-7, REMTECH, Inc., Huntsville, Alabama, December 1978.

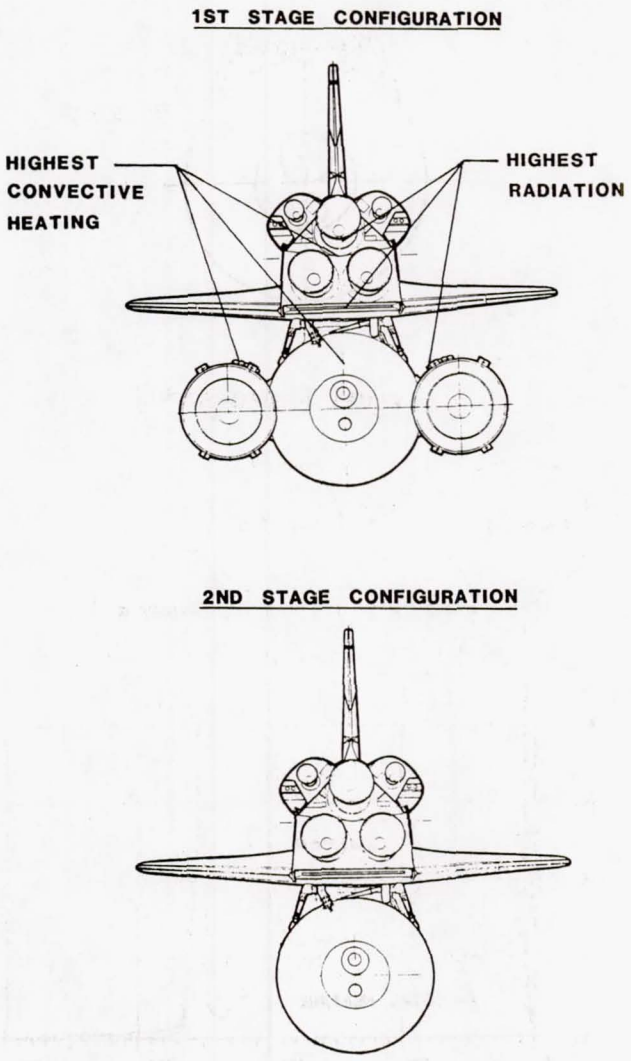

Figure 1.- Shuttle base configuration.

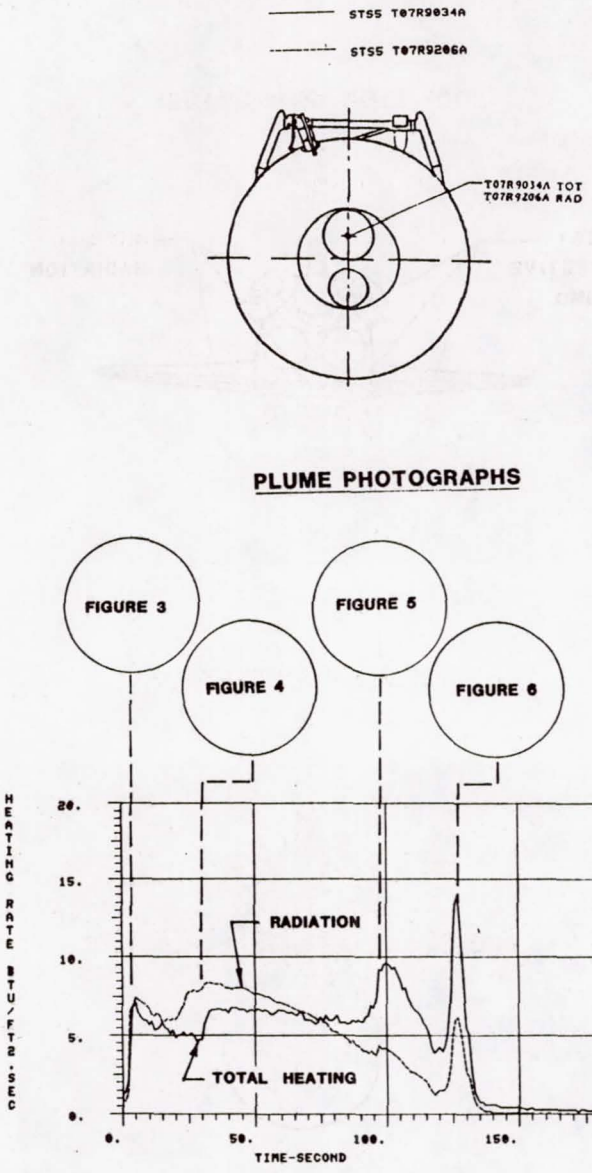

Figure 2.- Typical first-stage ascent base heating environment.

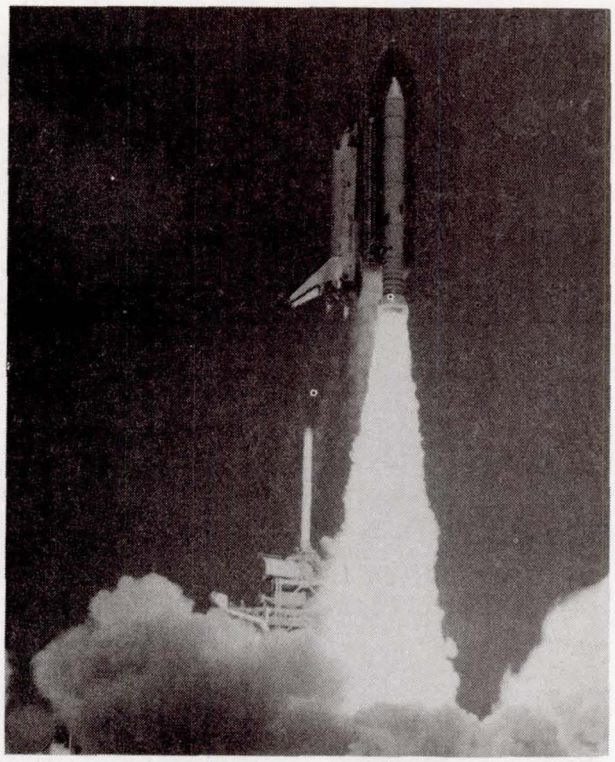

Figure 3.- Shuttle exhaust plumes at liftoff.

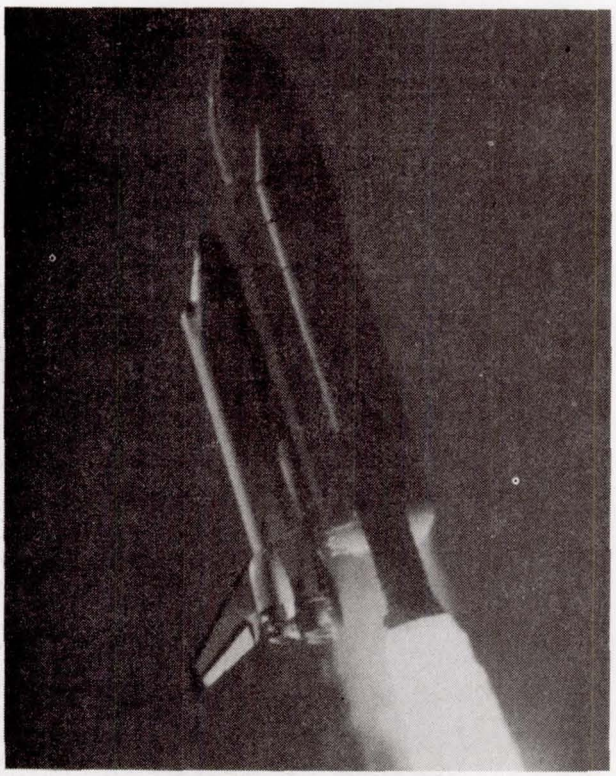

Figure 4.- Shuttle exhaust plumes at 7500 ft.

Figure 5.- Shuttle exhaust plumes at 90,000 ft.

Figure 6.- Shuttle exhaust plumes at 166,000 ft.

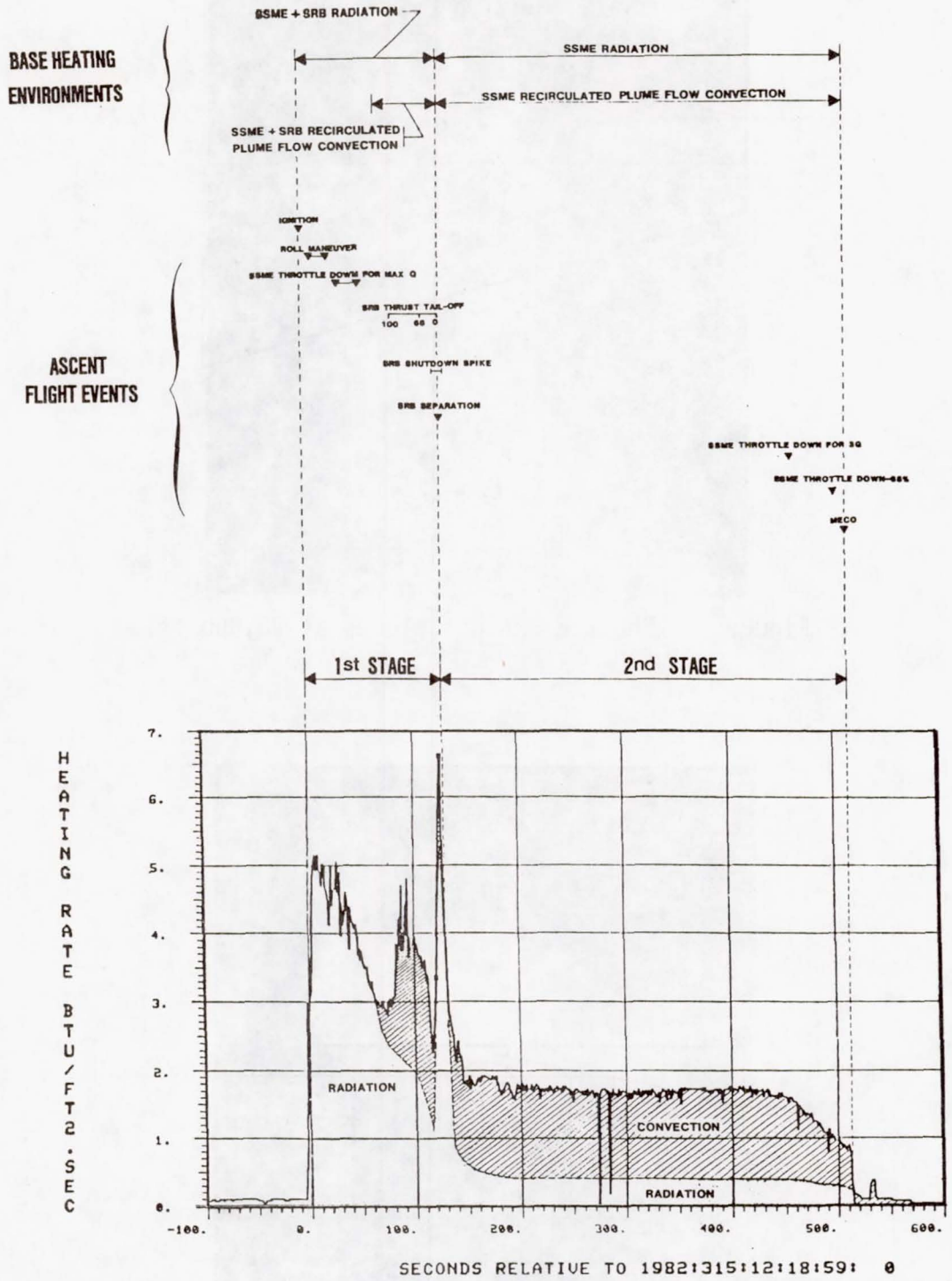

Figure 7.- Ascent flight events - typical orbiter heat shield environment.

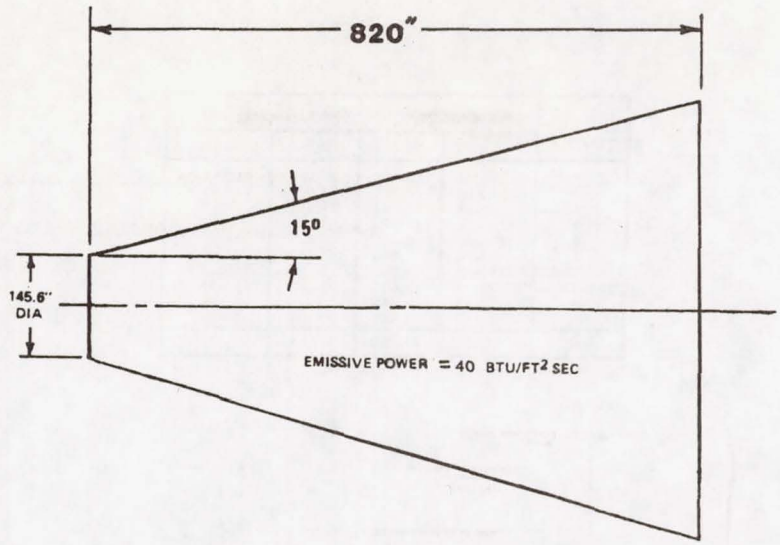

(a) Original model (ref. 2).

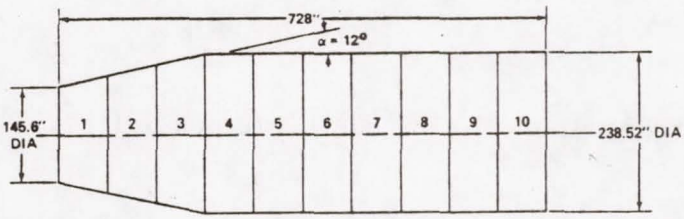

1	2	3	4	5	6	7	8	9	10	NUMBER
61	57	53	49	45	41	37	32	28	21	EMISSIVE POWER (BTU/FT² SEC)

(b) 1979 design model (ref. 3).

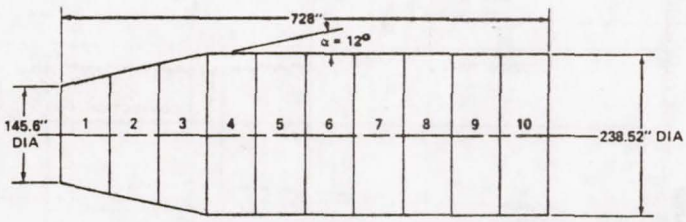

1	2	3	4	5	6	7	8	9	10	NUMBER
70	**59**	**57**	**53**	45	41	37	32	28	21	EMISSIVE POWER (BTU/FT² SEC)

(c) 1980 up-dated design model (ref. 4).

Figure 8.- SRM sea-level plume radiation models.

SRB PLUME MODEL EMISSIVE POWERS VS ALTITUDE

No.	Altitude/Emissive Power (Btu/ft^2-sec)			
	42 Kft	72 Kft	102 Kft	136 Kft
1	36.990	32.731	29.586	23.763
2	32.850	24.306	17.963	14.696
3	26.880	16.394	11.183	7.947
4	22.472	12.190	7.635	5.093
5	17.566	9.216	5.669	3.334
6	13.654	6.500	4.031	2.212
7	11.507	5.040	3.065	1.449
8	8.397	3.621	1.945	1.103
9	5.625	2.256	1.403	0.715
10	3.143	1.628	0.800	0.456
α	27.50	33.000	37.000	40.000

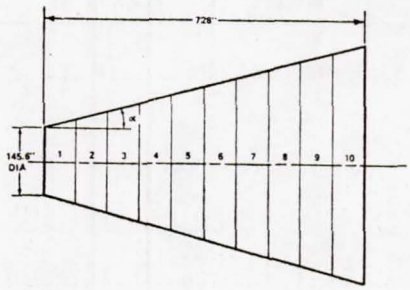

Figure 9.- SRM altitude plume model (ref. 7).

GEOMETRY AND EMISSIVE POWER OF THE SSME SEA LEVEL PLUME MODEL

SURFACE		Z-INCHES	R-INCHES	EMISSIVE POWER BTU/FT^2 - SEC
4° CONE		0 - 800	45-101	10-TRANSPARENT
CYLINDER		800-1800	100	10 ↓
DISK	1	60	30	70-OPAQUE
	2	100	30-40	60
	3	200	40-50	100
CYLINDER	1	60-100	30	40
	2	100-200	40	50
	3	200-800	50	50
	4	800-1800	50	30

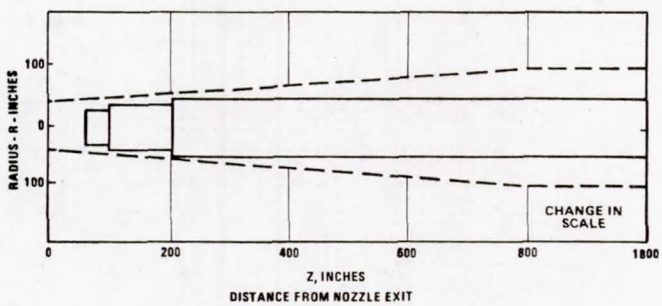

Figure 10.- SSME sea-level plume model (ref. 8).

FIRST STAGE WIND TUNNEL TESTS

TEST	FACILITY	MACH NO.	NO. OF RUNS	MEASUREMENTS PER RUN	TIME PERIOD
IH-5	CALSPAN LUDWIEG TUBE	4.5	46	36	JAN-JULY 1974
IH-34	LEWIS 10X10	$\leq$3.5	36	98	JUNE - AUG 1975
IH-39	LEWIS 10X10	$\leq$3.5	163	136	OCT, 1976 APRIL, 1977
IH-75	CALSPAN LUDWEIG TUBE	3.5 AND 4.5	50	100	FALL, 1977

SECOND STAGE VACUUM TANK TESTS

TEST	FACILITY	NO. OF RUNS	MEASUREMENTS PER RUN	TIME PERIOD
OH-3	MSFC IBFF	38	24	MAY-AUG 1974
OH-64	LEWIS PLUM BROOK SPACE POWER	154	162	APRIL-JUNE 1975
OH-78	JSC CHAMBER A	266	179	JULY-NOV 1976
OH-79	JSC CHAMBER A	OPEN	OPEN	SPRING, 1978

Figure 11.- Shuttle base heating test program.

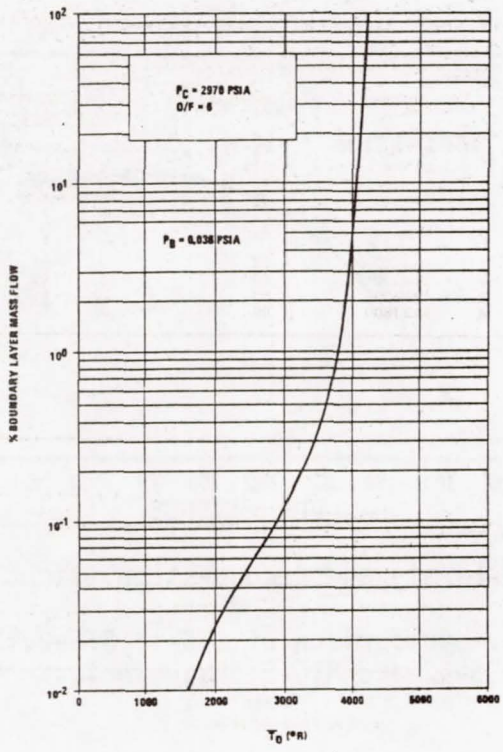

Figure 12.- Mass-averaged total temperature at the nozzle exit plane of the Space Shuttle orbiter main engine (ref. 1).

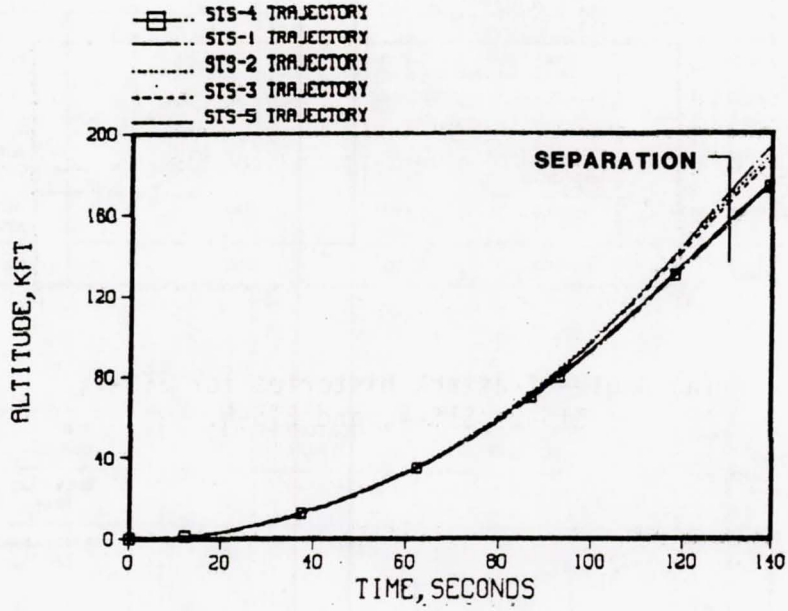

(a) First-stage flight.

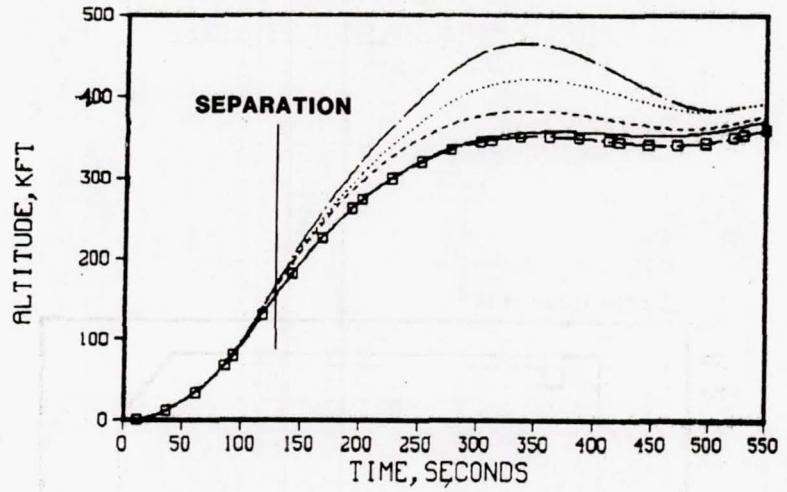

(b) First- and second-stage flight.

Figure 13.- Comparison of STS-1, STS-2, STS-3, STS-4, and STS-5 trajectories.

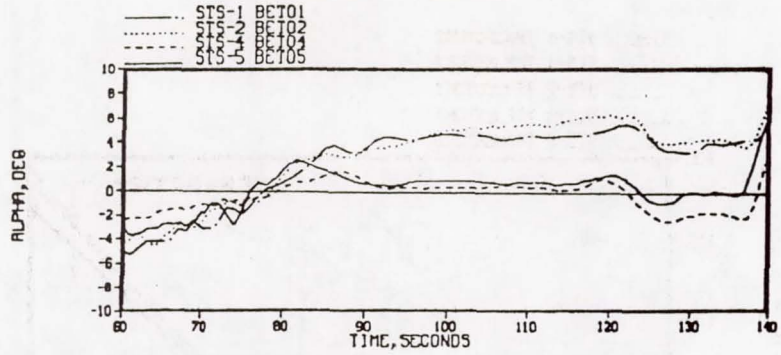

(a) Angle-of-attack histories for STS-1, STS-2, STS-4, and STS-5.

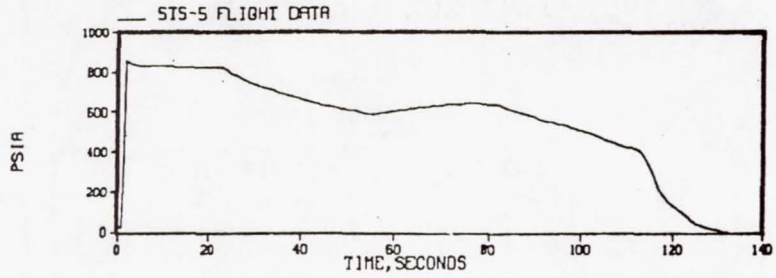

(b) R-SRB chamber pressure.

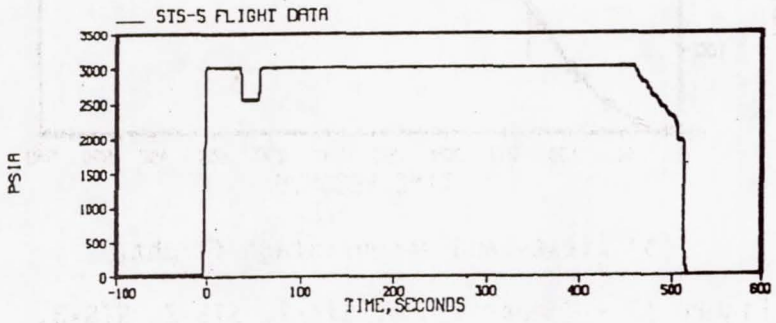

(c) SSME-3 chamber pressure.

Figure 14.- Flight parameters.

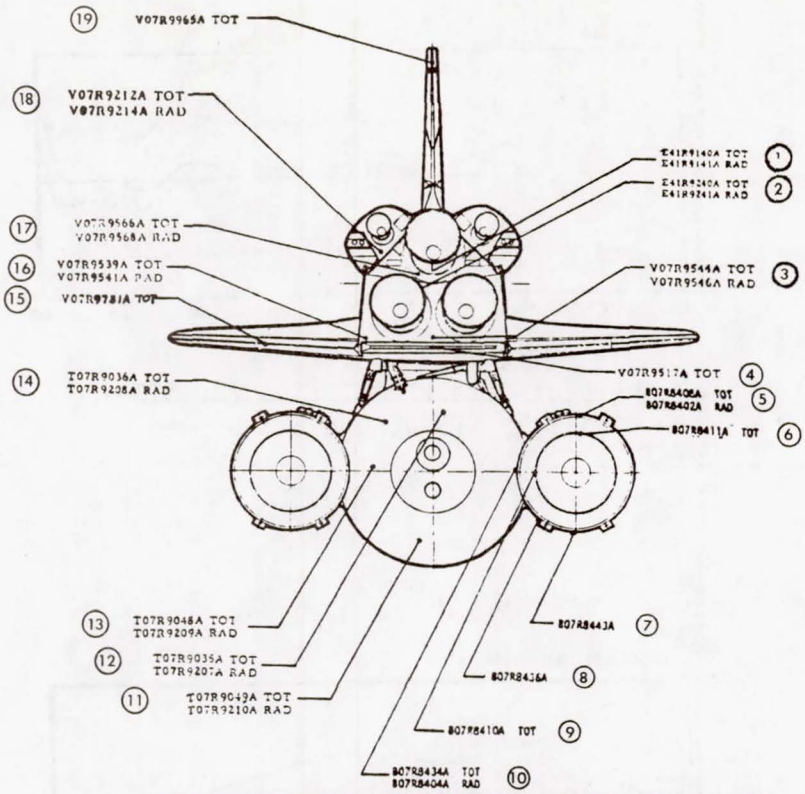

COMPONENT	LOC	HEATING RATE, BTU/FT.^{2} SEC								FLIGHT DATA
		10 SEC (780 FT)		100 SEC (98,000 FT)		126 SEC (158,500 FT)		300 SEC (409,000 FT)		
		RAD	TOT	RAD	TOT	RAD	TOT	RAD	TOT	
ORBITER										
HEAT SHIELD	③	5.10	3.70	2.70	4.75	4.85	6.10	0.30	1.00	
	⑯	4.65	2.85	2.40	3.95	5.10	5.12	0.10	0.30	
	⑰	4.00	2.70	1.70	4.15	2.91	4.38	0.30	1.55	
OMS POD	⑱	5.10	5.10	2.20	3.75	3.40	3.95	0.70	1.40	
VERTICAL TAIL	⑲	--	9.20	--	5.05	--	15.20	--	0.50	FIG. 20
ELEVON	⑮	--	5.20	--	4.00	--	8.25	--	0.10	FIG. 19
BODYFLAP	④	--	13.25	--	10.60	--	23.60	--	1.00	FIG. 18
SSME #1	①	9.00	13.25	3.20	9.05	11.23	26.80	0.80	2.50	FIG. 21
SSME #2	②	8.30	9.60	2.35	10.20	2.05	5.20	0.80	3.20	
RSRB										
NOZZLE	⑥	--	5.00	--	4.35	--	7.60			
	⑨	--	10.75	--	8.50	--	19.50*			
AFT SKIRT	⑤	8.50	11.40	1.85	5.20	7.00	15.40			FIG. 23
	⑦	--	0.10	--	1.35	--	2.60			
	⑧	--	0.70	--	2.65	--	6.30*			
	⑩	6.00	3.80	3.40	7.30	7.60	11.30*			
ET AFT DOME	⑪	3.55	3.00	1.85	3.95	2.75	8.30	0.00	0.00	
	⑫	3.50	3.80	2.10	5.30	6.35	11.70	0.00	0.00	FIG. 22
	⑬	3.00	4.60	1.75	6.50	3.55	12.10	0.00	0.00	
	⑭	2.55	5.00	1.25	6.35	3.60	14.05	0.00	0.00	

*OFFSCALE

Figure 15.- Base heating environment distribution.

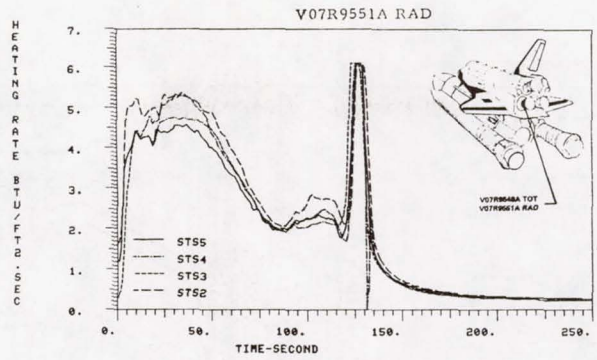

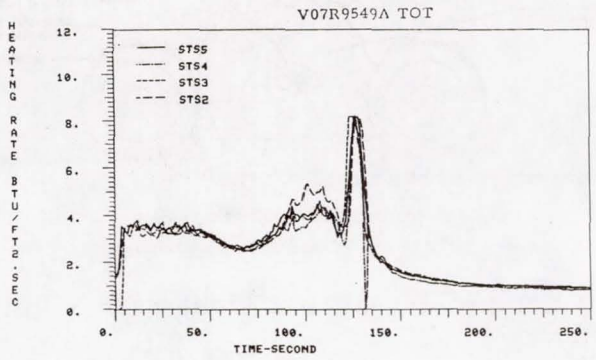

Figure 16.- Typical Shuttle flight data - orbiter heat shield.

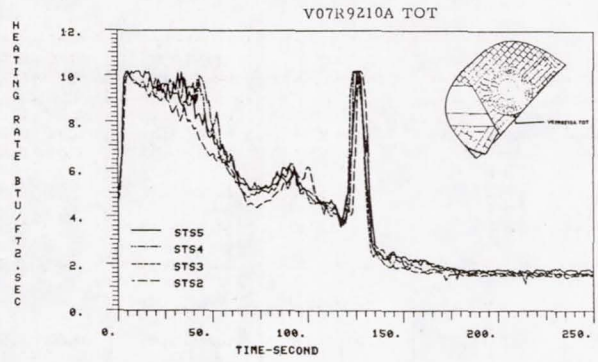

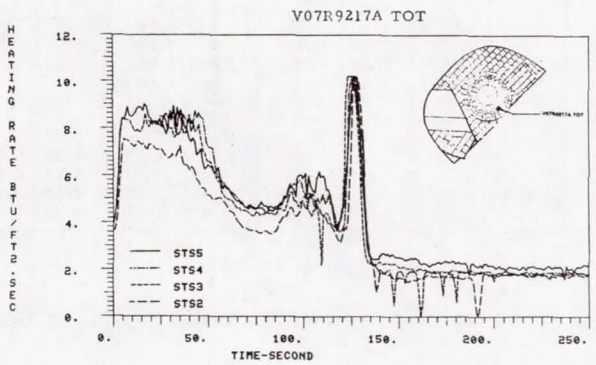

Figure 17.- Typical Shuttle flight data - OMS pod.

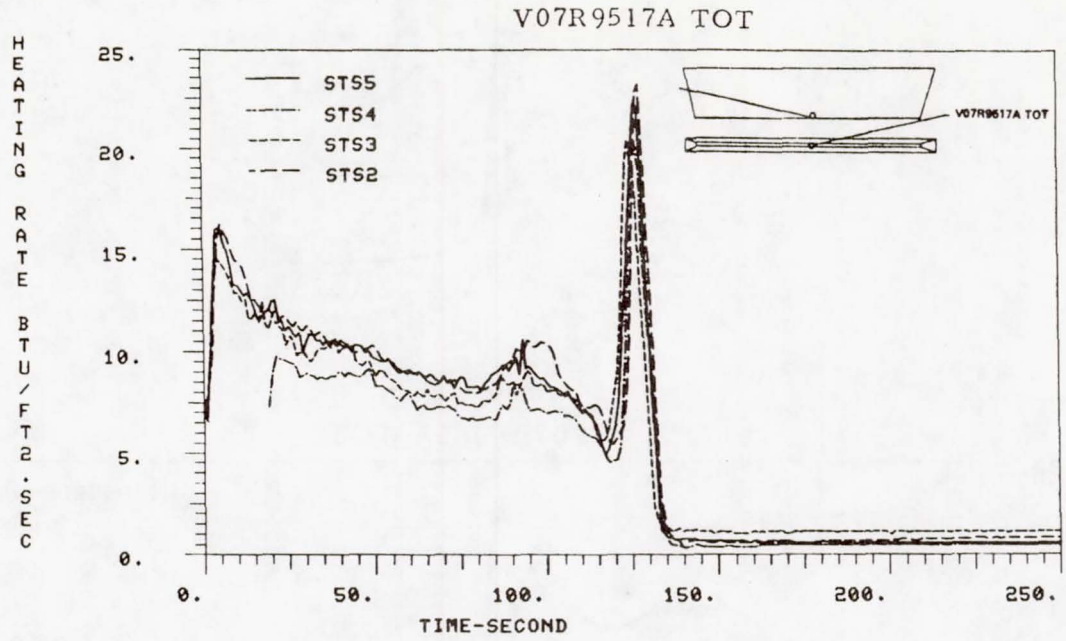

Figure 18.- Typical Shuttle flight data - body flap.

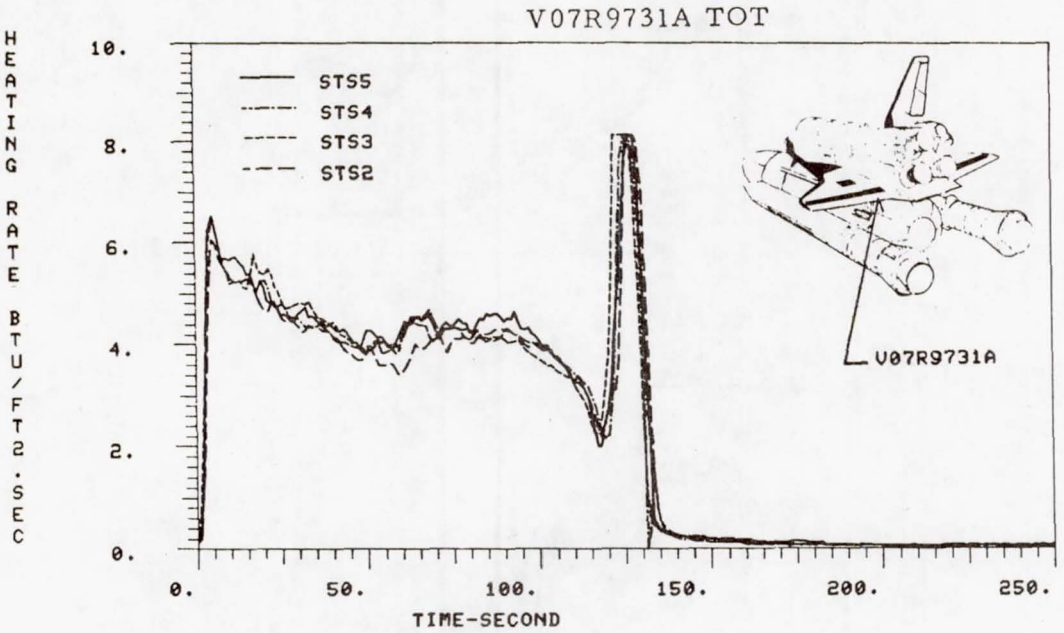

Figure 19.- Typical Shuttle flight data - elevon.

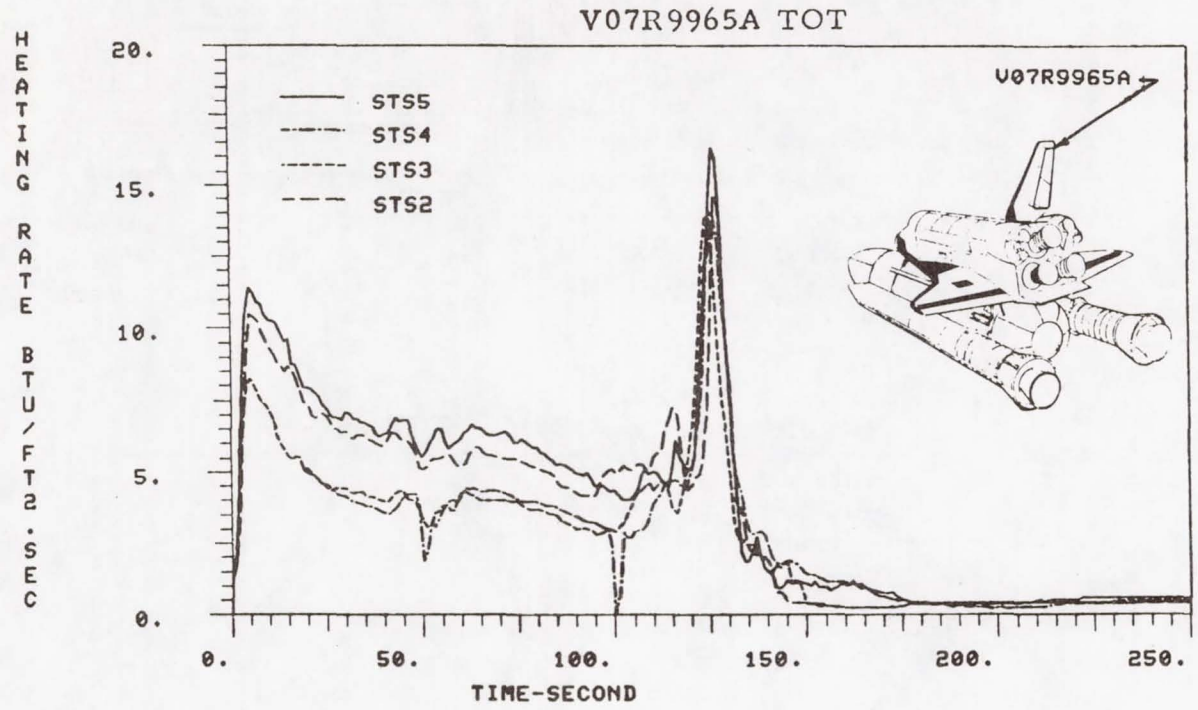

Figure 20.- Typical Shuttle flight data - vertical tail.

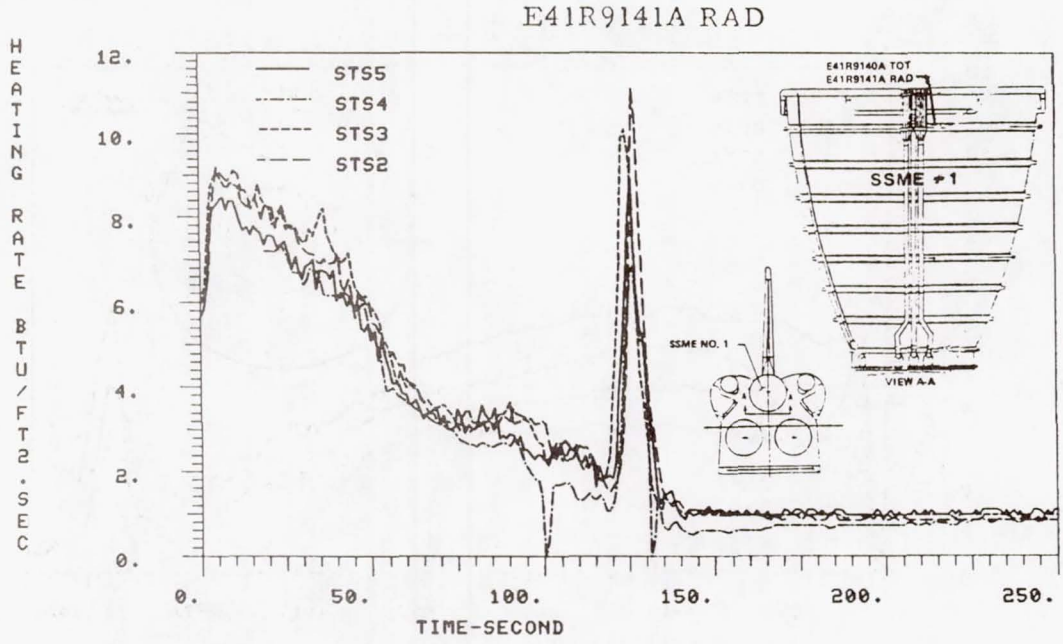

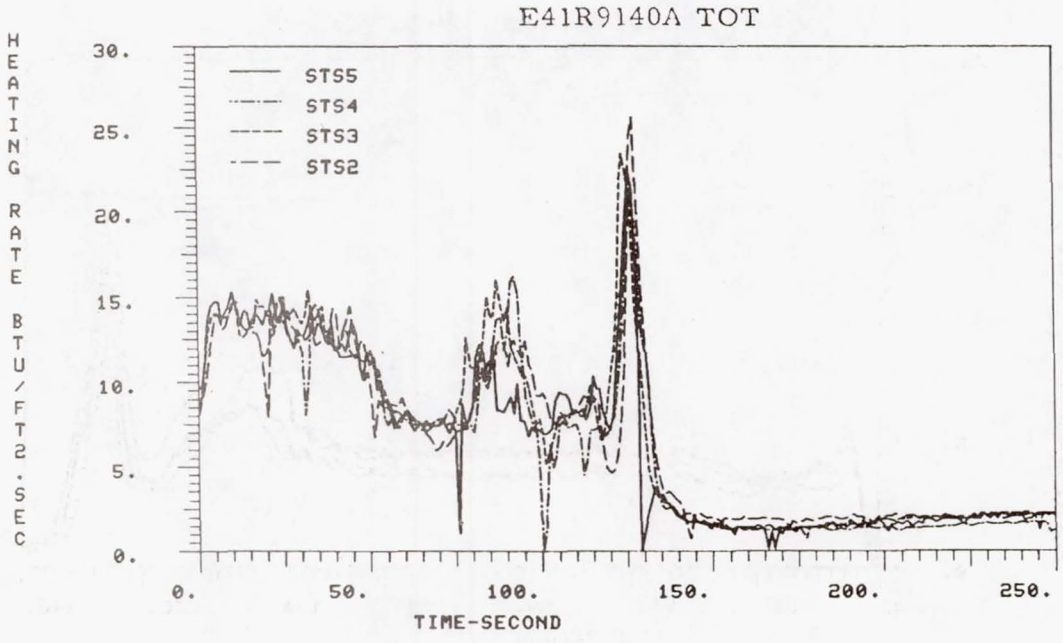

Figure 21.- Typical Shuttle flight data - SSME number 1.

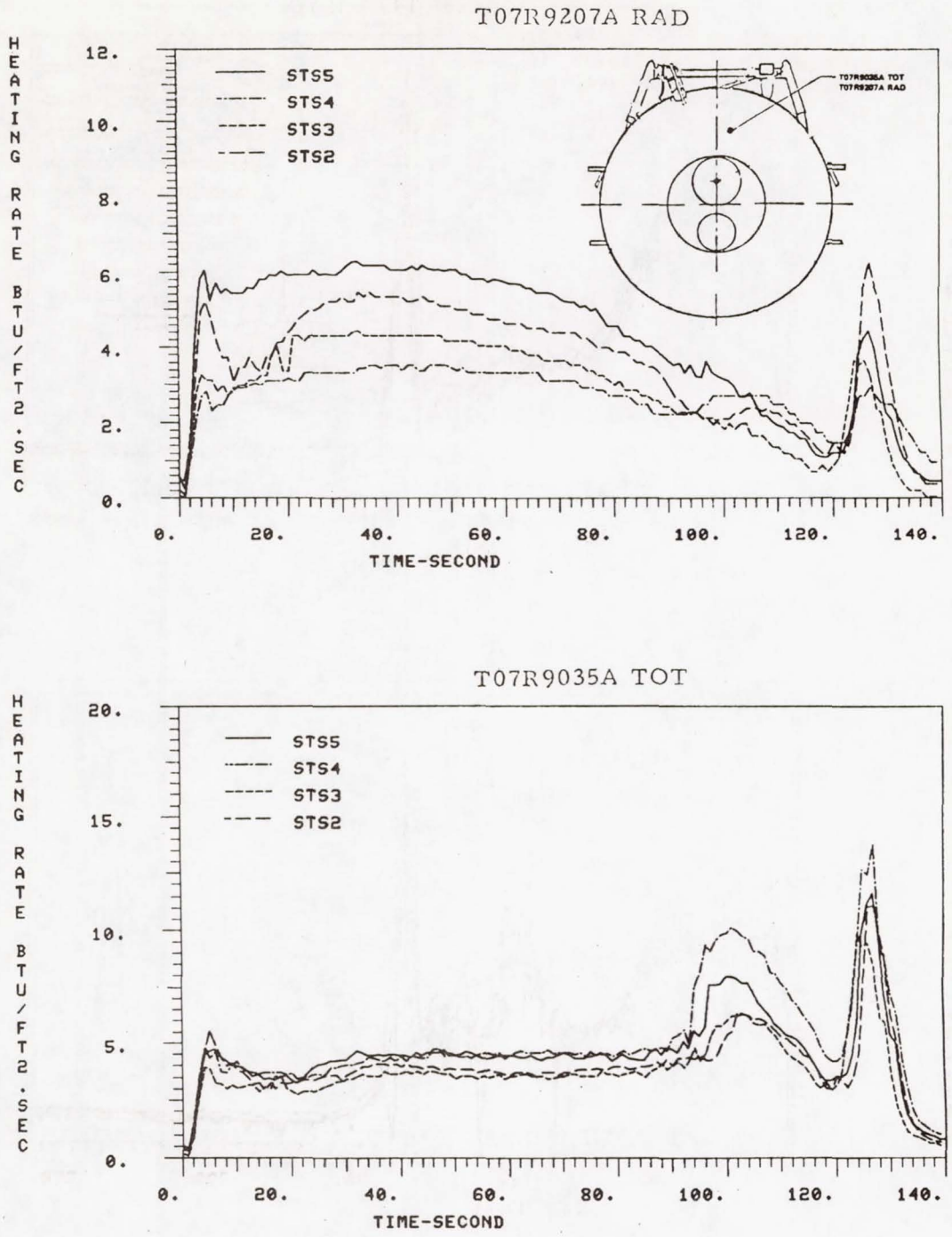

Figure 22.- Typical Shuttle flight data - external LH_2 tank aft dome.

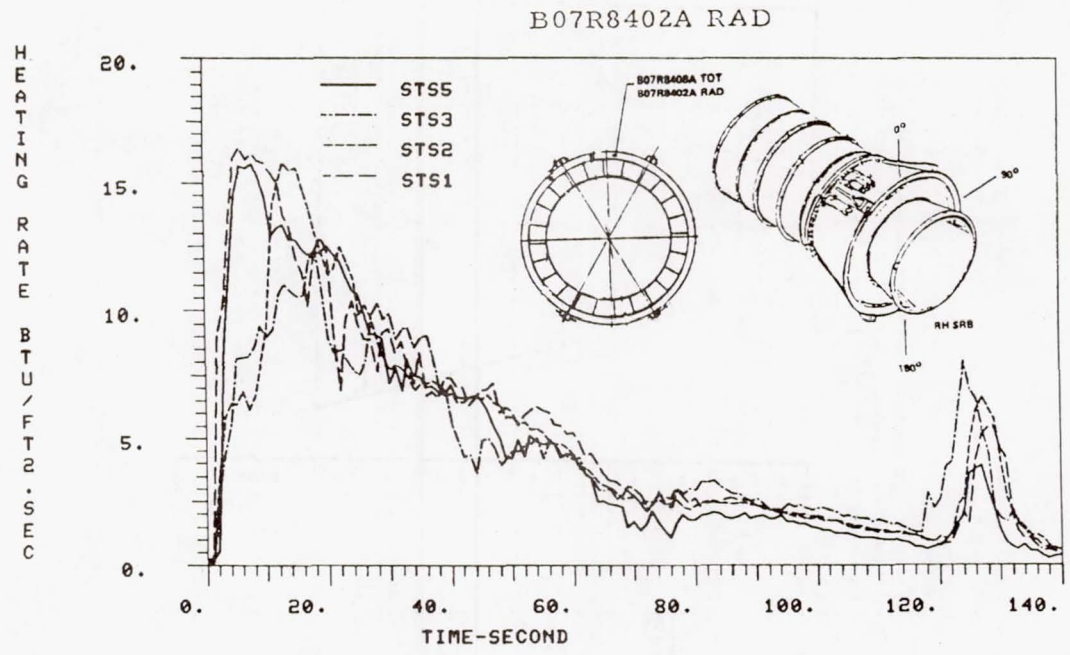

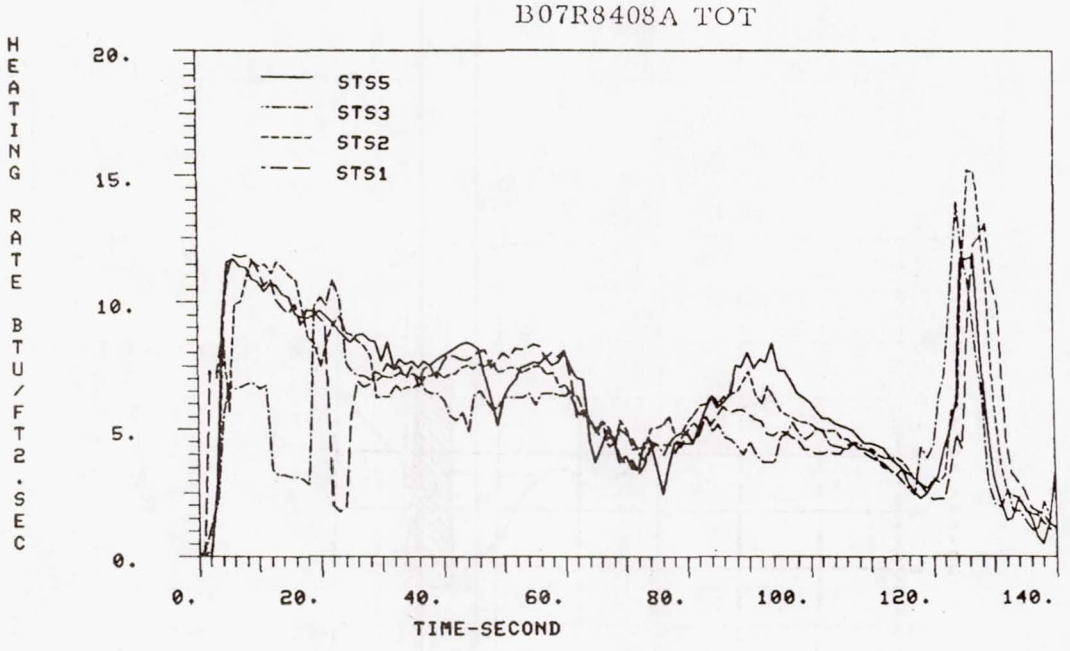

Figure 23.- Typical Shuttle flight data - right SRB aft skirt.

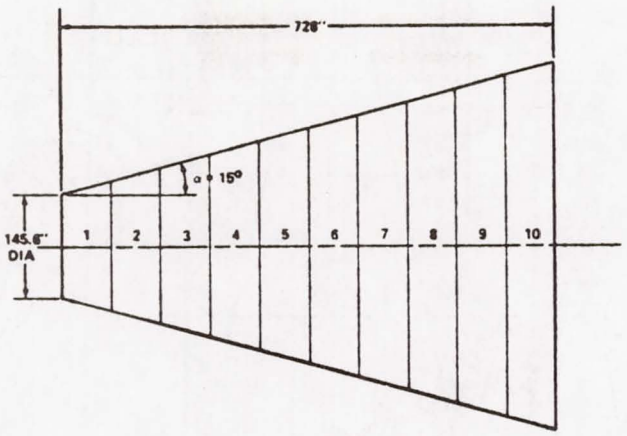

1	2	3	4	5	6	7	8	9	10	NUMBER
70	59	57	53	45	41	37	32	28	21	EMISSIVE POWER (BTU/FT^2 SEC)

Figure 24.- Current SRM sea-level plume radiation model (ref. 14).

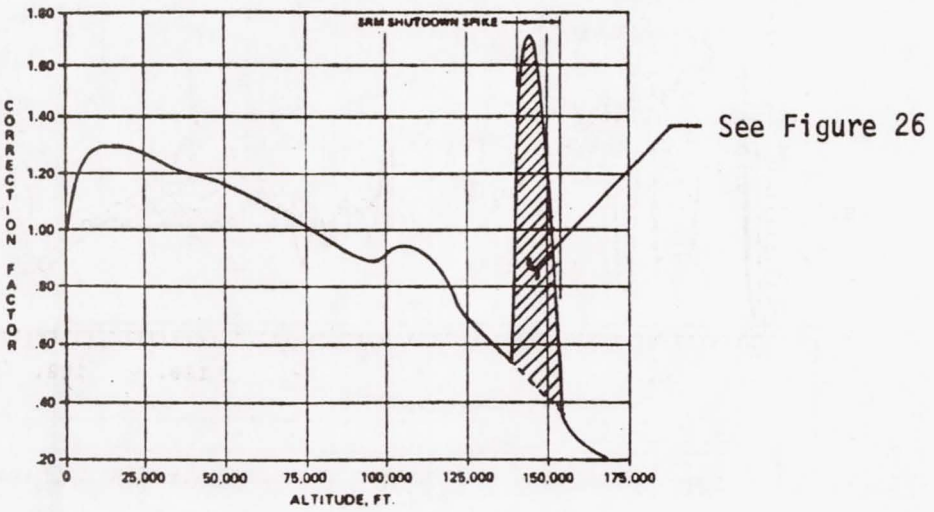

Figure 25.- SRM altitude correction factor (ref. 14).

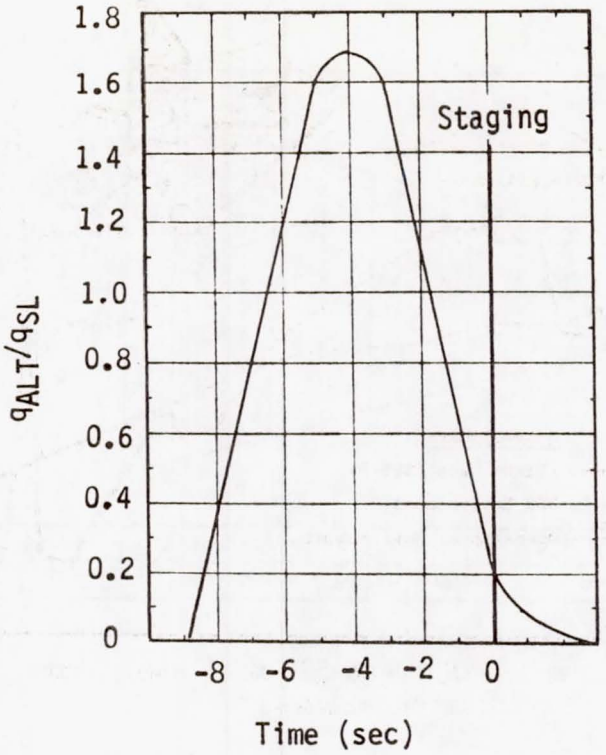

Figure 26.- SRM shutdown radiation spike (ref. 14).

SHAPE	EMISSIVE POWER BTU/FT^2–SEC	DISTANCE FROM EXIT INCHES	RADIUS INCHES
DISK 1 – TRANSPARENT	150	50	25
2 – TRANSPARENT	120	350	20–50
CYLINDER 1 – OPAQUE	60	50–350	20
2 – OPAQUE	60	300–600	50
3 – OPAQUE	40	600–1200	50
CONE – TRANSPARENT	12	100–1100	40–120

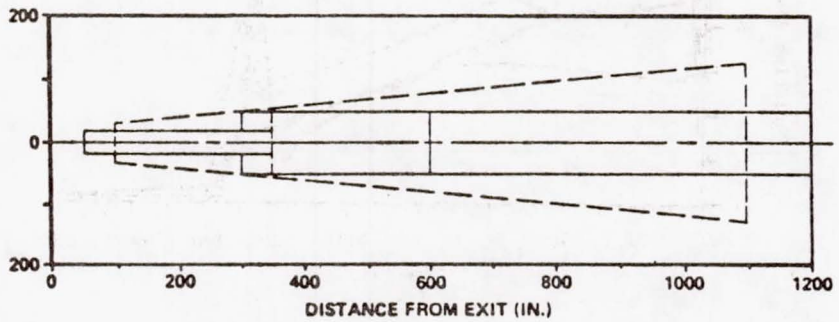

Figure 27.- Current SSME sea-level plume radiation model (ref. 15).

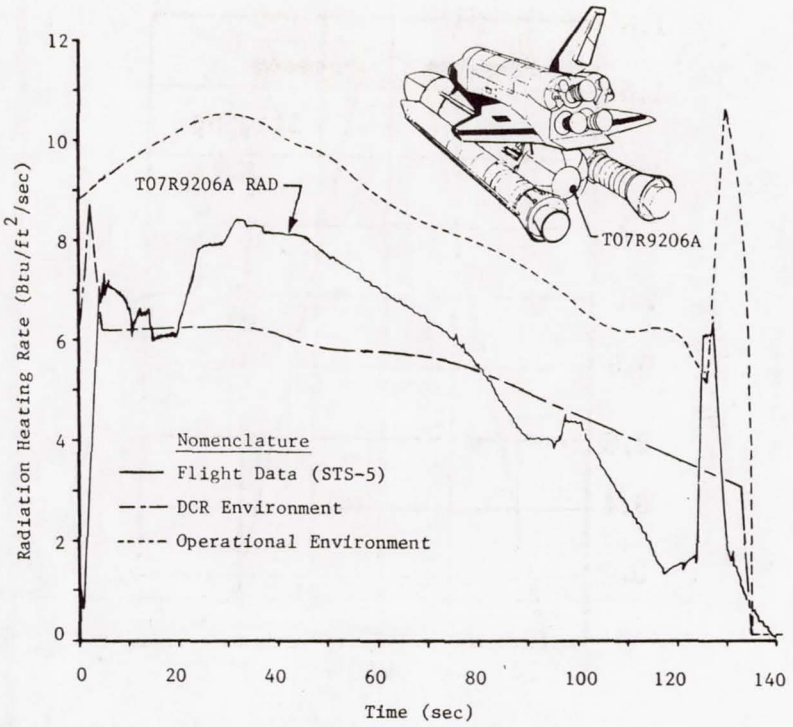

Figure 28.- External tank radiation base heating.

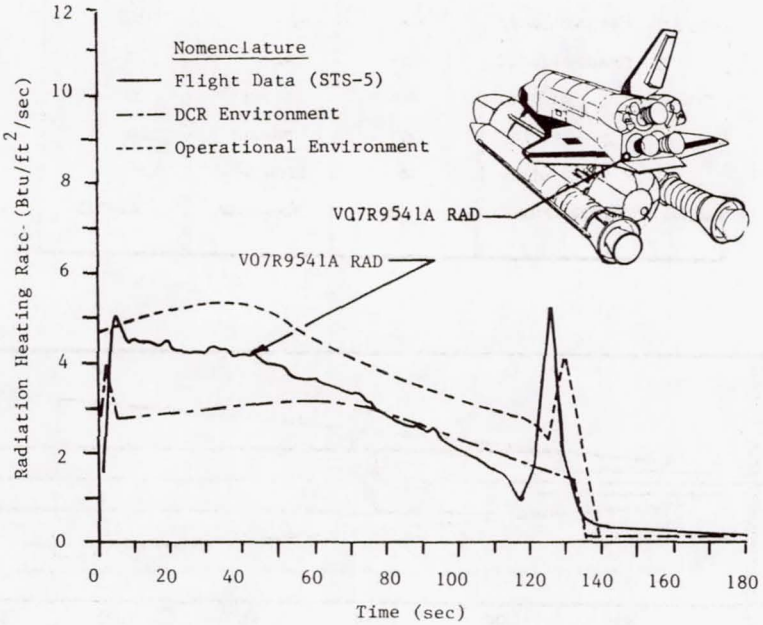

Figure 29.- Orbiter heat shield radiation base heating.

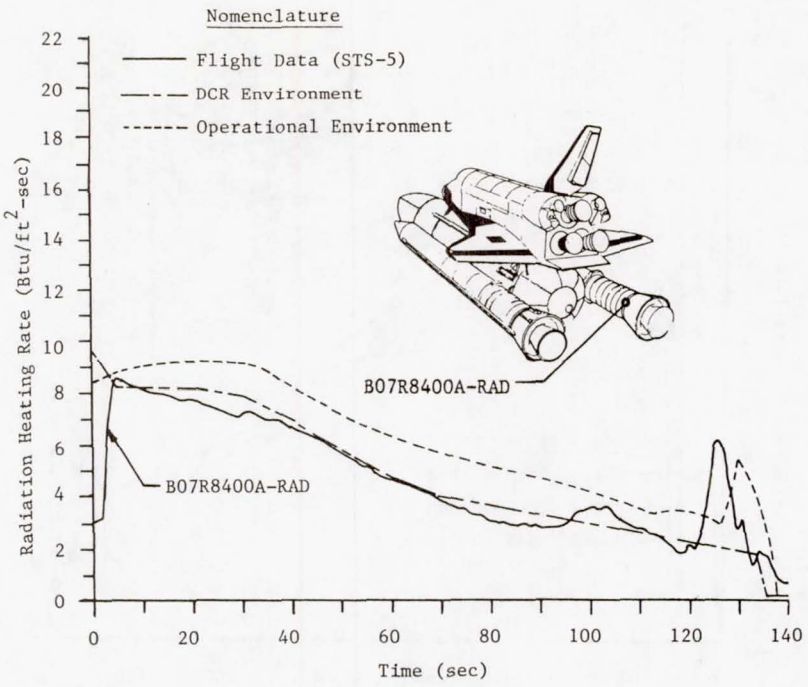

Figure 30.- SRB kick ring radiation base heating.

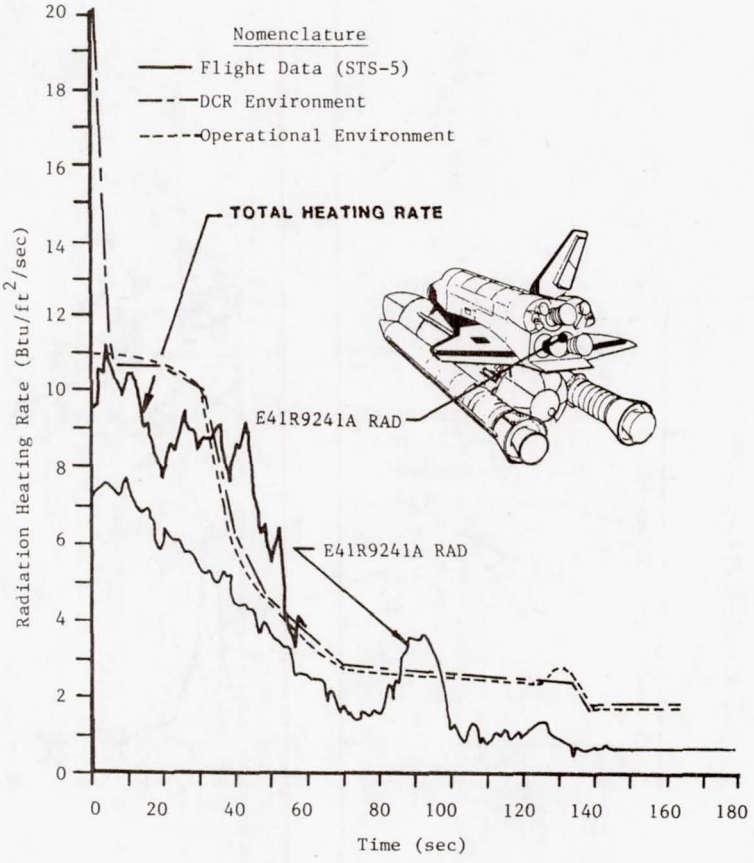

Figure 31.- SSME number 2 radiation base heating.

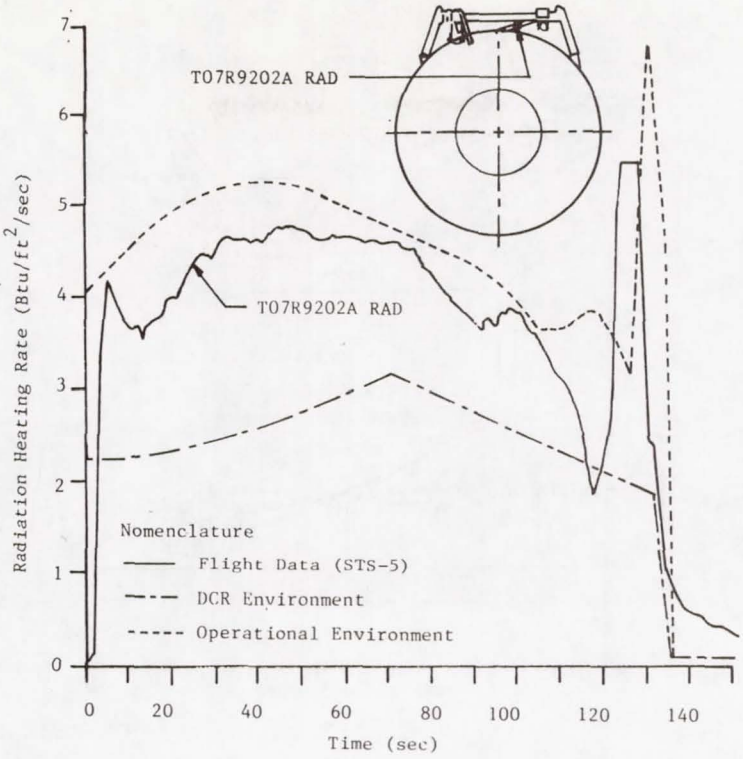

Figure 32.- ET/orbiter attach structure radiation base heating.

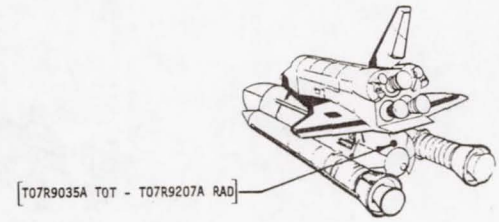

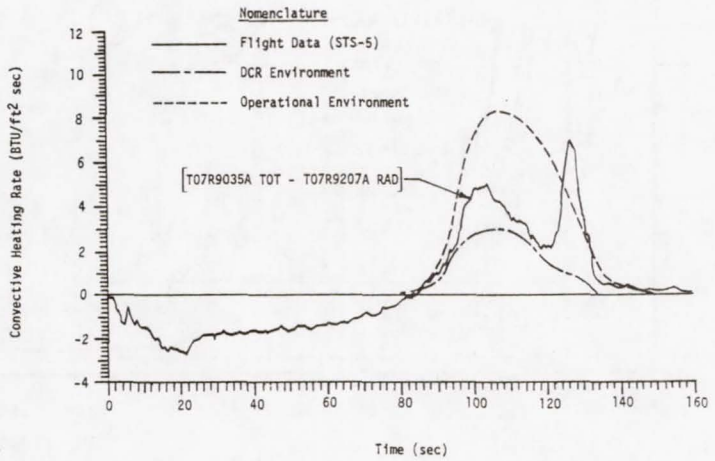

Figure 33.- External tank convective base heating.

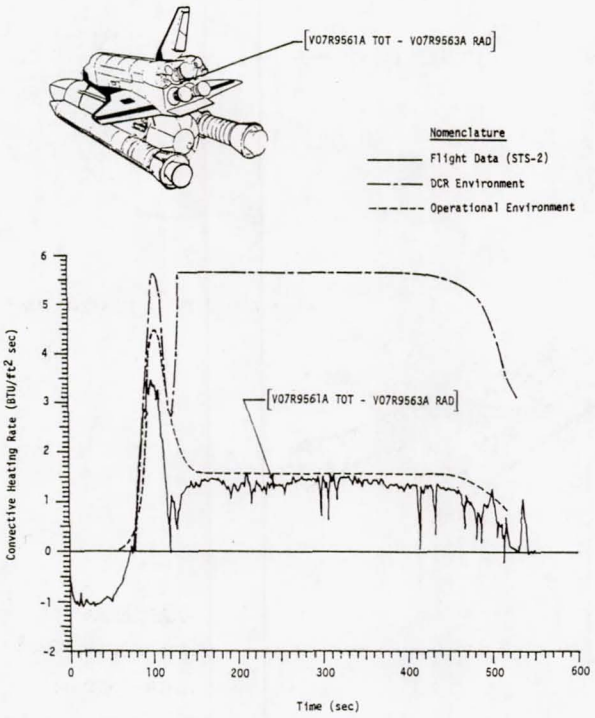

Figure 34.- Orbiter heat shield convective base heating.

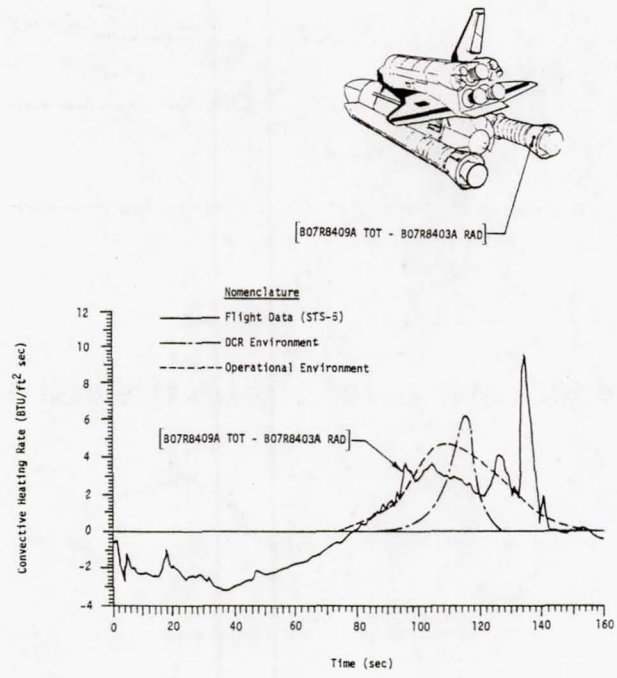

Figure 35.- SRB aft skirt convective base heating.

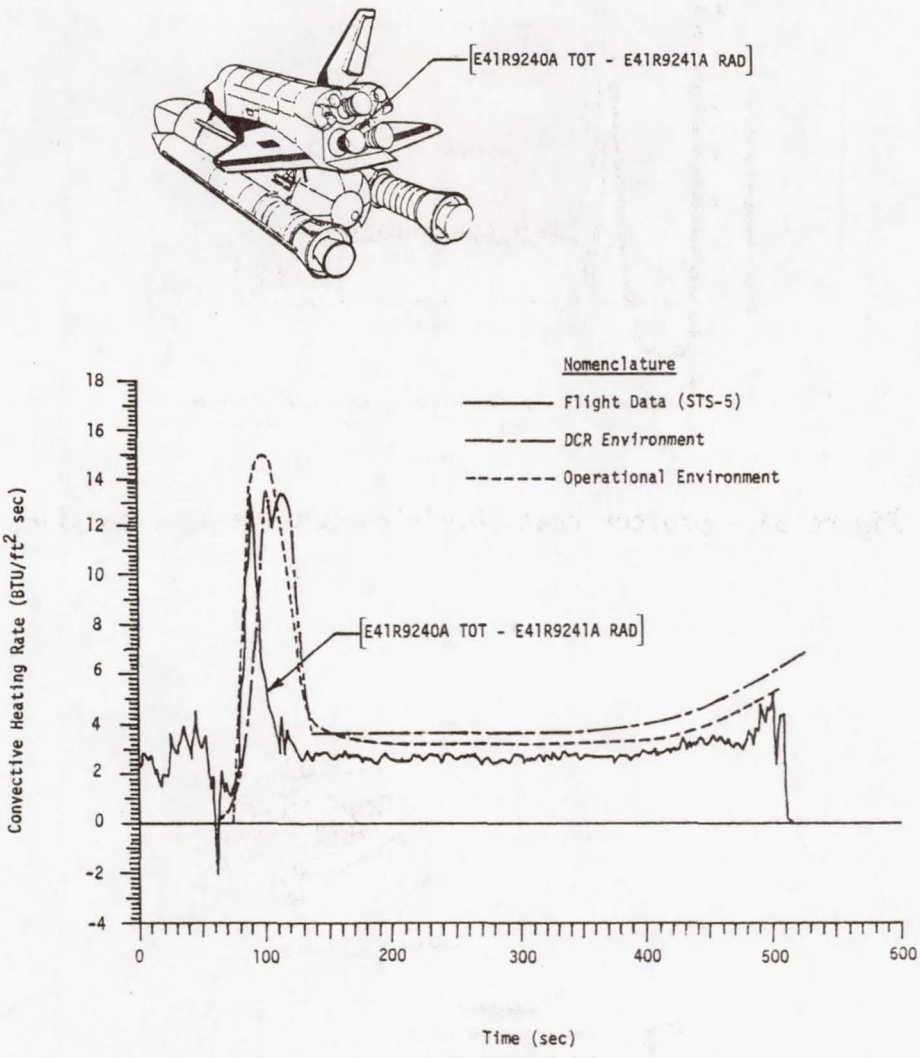

Figure 36.- SSME number 2 convective base heating.